RESEARCH ARTICLE

National Science Review
6: 713–718, 2019
doi: 10.1093/nsr/nwz061
Advance access publication 9 May 2019

PHYSICS

High-temperature superconductivity in sulfur hydride evidenced by alternating-current magnetic susceptibility

Xiaoli Huang[1,†], Xin Wang[1,†], Defang Duan[1], Bertil Sundqvist[1,2], Xin Li[1], Yanping Huang[1], Hongyu Yu[1], Fangfei Li[1], Qiang Zhou[1], Bingbing Liu[1] and Tian Cui[1,*]

ABSTRACT

The search for high-temperature superconductivity is one of the research frontiers in physics. In the sulfur hydride system, an extremely high T_c (∼200 K) has been recently developed at pressure. However, the Meissner effect measurement above megabar pressures is still a great challenge. Here, we report the superconductivity identification of sulfur hydride at pressure, employing an *in situ* alternating-current magnetic susceptibility technique. We determine the superconducting phase diagram, finding that superconductivity suddenly appears at 117 GPa and T_c reaches 183 K at 149 GPa before decreasing monotonically with increasing pressure. By means of theoretical calculations, we elucidate the variation of T_c in the low-pressure region in terms of the changing stoichiometry of sulfur hydride and the further decrease in T_c owing to a drop in the electron–phonon interaction parameter λ. This work provides a new insight into clarifying superconducting phenomena and anchoring the superconducting phase diagram in the hydrides.

Keywords: high pressure, hydrides, superconductivity, Meissner effect

INTRODUCTION

Since the discovery of superconductivity slightly more than a century ago [1], the quest for ever-higher critical temperatures, T_c, has remained a great challenge and an important topic for both experimental and theoretical research. Because of their high Debye temperatures and chemical precompression, some hydrides have been predicted theoretically as good candidates to realize high-temperature superconductivity at pressures lower than those expected for metallic hydrogen [2–6]. However, the field showed no significant experimental breakthroughs for a very long time [7–9], until superconductivity was observed in a newly discovered hydrogen sulfide system with a record superconducting transition temperature T_c of 200 K [10], exceeding the highest values found in the cuprates [11–13]. The transition into superconductivity was indicated by a sharp drop of the resistance to zero and confirmed by a strong isotope effect in D_2S [14,15]. The superconducting state was associated with a phase transformation and decomposition of H_2S to H_3S+S [16]. These results have kindled an intense search for room-temperature superconductivity in hydrogen-dominated compounds.

The Meissner effect is not only the essential method to identify the superconducting state of materials, but it also plays a crucial role in our understanding of the mechanism of high-temperature superconductivity. In contrast to the zero-resistance state, Meissner effect experiments are relatively more difficult to fulfill in the sulfur hydride superconducting system above megabar pressures. Drozdov *et al.* have successfully probed the Meissner effect of a sulfur hydride sample at one pressure point 155 GPa by using a superconducting quantum interference device (SQUID) [15], though it is very difficult to realize the Meissner effect measurements in SQUID under such a high pressure [17]. A novel method, in which the magnetic field on a Sn sensor inside the H_2S sample was monitored by nuclear resonance scattering of synchrotron radiation, was

[1]State Key Laboratory of Superhard Materials, College of Physics, Jilin University, Changchun 130012, China and [2]Department of Physics, Umeå University, SE-90187 Umeå, Sweden

***Corresponding author.** E-mail: cuitian@jlu.edu.cn
[†]Equally contributed to this work.

Received 20 March 2019; **Revised** 24 April 2019; **Accepted** 8 May 2019

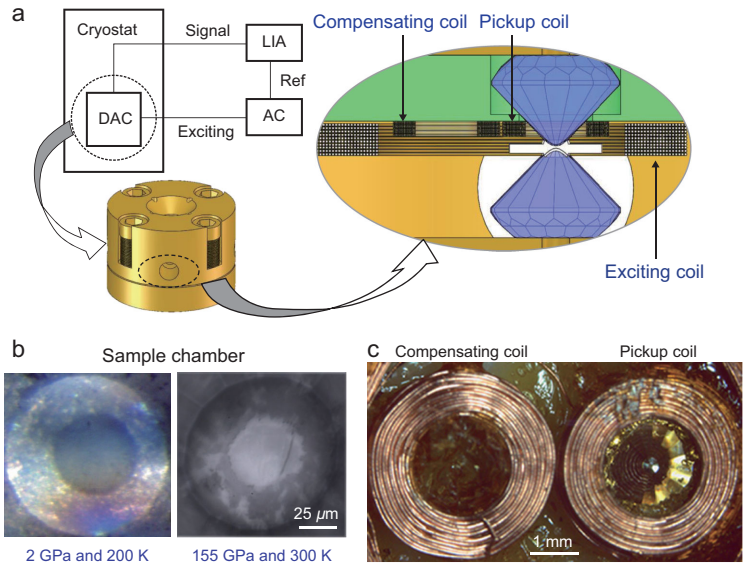

Figure 1. Schematic image of the experimental set-up for alternating-current magnetic susceptibility measurement. (a) Simplified flow chart for the magnetic susceptibility measurement set-up for the diamond anvil cell (DAC). LIA and AC denote lock-in amplifier and alternating-current source, respectively. (b) The sample in the gasket hole at 2 GPa and 200 K (left), and at 155 GPa and 300 K (right), respectively. (c) A pickup coil wound around a diamond anvil and a compensating coil connected in opposition.

developed to qualitatively detect the superconductivity at 153 GPa [18]. Significant experimental achievements have been made in the superconducting measurement of sulfur hydride, but some physical profiles remain vague, particularly regarding the exact superconducting temperature, and the way that the superconducting phase changes with pressure. Besides, as reported in the electrical resistance experiments, different compression routes will achieve various T_c in a sulfur hydride sample. Unfortunately, the reason why the compression route during cooling or warming greatly affects the superconducting T_c and the possible mechanisms behind this phenomenon are still unambiguous. Further superconductivity studies of sulfur hydride are thus greatly desirable. Here, we report measurements of the Meissner effect under variable pressure to map the superconducting diamagnetism and high-temperature superconducting state in the sulfur hydride system, using a highly sensitive magnetic susceptibility technique adapted for a megabar-pressure diamond anvil cell (DAC). Most importantly, we have unambiguously determined the superconducting phase diagram of the material from magnetic susceptibility data. The complementary theoretical calculations explain the variation of T_c as a function of pressure.

RESULTS AND DISCUSSION

All *in situ* high-pressure experiments shown in this study were carried out by using a symmetric DAC apparatus. Typically, we loaded H_2S into a glove box under an argon atmosphere, to guarantee an uncontaminated sample (see the section entitled 'Methods' in the online supplementary data). We have identified the characteristic molecular vibrations of the sample from Raman spectra. These are unambiguously consistent with the literature data [15] (Fig. S1, online supplementary data). In the conventional superconducting phase, the magnetic susceptibility is negative or the response to an external magnetic field is diamagnetic, as the sample enters the superconducting state. The protocol of the magnetic-susceptibility technique for measuring the superconductivity is described in previous works [19–21]. In the present work, we have optimized this technique to study samples in the megabar pressure range (Fig. 1a). The target sample was loaded into the hole of the non-magnetic gasket at about 2.0 GPa and 200 K, and a typical sample chamber at 155 GPa and 300 K is shown in Fig. 1b. The detailed compression routes of the current work can be found in the online supplementary data. The alternating-current susceptibility was detected with a lock-in amplifier (LIA). The signal coil is wound around one of the diamond anvils with a compensating coil connected in opposition (Fig. 1c). This is essential for obtaining a good discernable signal. The value of T_c is taken to be the onset of superconductivity, defined by the intersection of a line drawn through the steep slope of the curve and the region of zero slope above the transition.

We have performed three experimental runs studying the superconducting state of compressed H_2S samples, as shown in Fig. 2. In the first run the sample was compressed up to 149 GPa, above which the diamond failed. On this occasion, no superconducting response was observed below 100 GPa, but a characteristic transition into the superconducting state emerged at 117 GPa (Fig. 2a). The T_c, identified as the onset of the steep drop, was found to be 38 K. With increasing pressure, significantly higher values for T_c were found. At 130 GPa, the superconducting onset temperature is 55 K (Fig. 2b). The pressure was then increased to 149 GPa at 300 K, where the sample was kept for about seven days, waiting out the possible transition kinetics in the H_3S phase that was formed, as reported in previous works [14,15,22]. When the temperature was finally decreased at this pressure, the superconducting transition was observed at 183 K (Fig. 2c), which is qualitatively compatible with our previous theoretical predictions [10]. In the second run, the

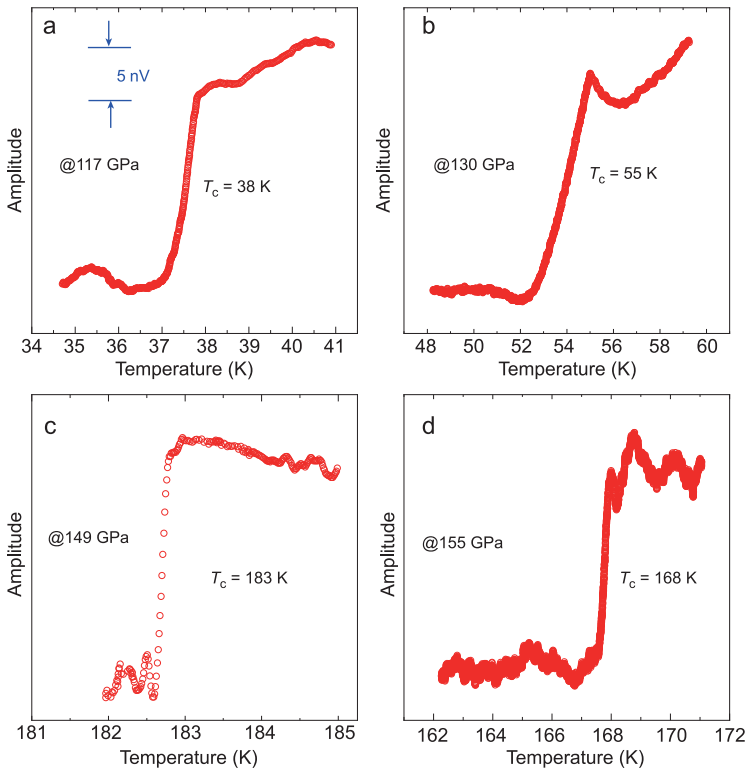

Figure 2. Magnetic susceptibility signals of sulfur hydride at various pressures. Curves show typical amplitude records from the coil system during each temperature scan at (a) 117 GPa, (b) 130 GPa, (c) 149 GPa and (d) 155 GPa. To obtain the strong amplitude signal, we kept the sample and compensating coil signals in phase. The critical temperature T_c is estimated from the onset of the superconducting transition.

target pressure range was from 155–171 GPa. A well-defined and reproducible superconducting signal was triggered at about 168 K at 155 GPa (Fig. 2d). When the pressure was increased further, there was an abrupt decrease in T_c, which shifted down to 140 K at 171 GPa. In the third run, we first applied 130 GPa on the sample at temperatures $T <$ 100 K. Upon cooling the sample, at 130 GPa, the superconducting transition appeared at about 55 K. Thereafter, the sample was rapidly warmed to 300 K with the pressure maintained at 130 GPa. Upon further compression, the superconducting transition appeared at about 173 K and 168 K at 143 GPa and 155 GPa, respectively. The variation tendency of T_c with pressure is identical with the first and second runs. However, when the sample was compressed up to 170 GPa, the diamond failed.

To shed further insight on the pressure dependence of T_c in the high-temperature superconducting sulfur hydride system, we have plotted our experimental data together with all previous experimental measurements and our previous theoretical calculations (Fig. 3a) [10,14,15,22]. The uncertainties in determining T_c are especially large above 150 GPa. To reach ultrahigh pressure the diameter of the diamond anvil culets is reduced, leading to a reduction of the magnetic signal that is proportional to the volume of the sample [23]. The signal-to-noise ratio is thus reduced, resulting in the larger uncertainty in T_c upon further compression. A close study of Fig. 3a shows that there is a pronounced kink in the pressure dependence of T_c at about 149 GPa, and the diagram can be divided into two regions. Below 130 GPa the onset temperature T_c is lower than 100 K, which was also observed in the reported electrical resistance measurements [14]. Near 149 GPa high-T_c superconductivity appears and simultaneously the H_3S phase becomes the dominant component in the sample, as shown by the reported X-ray diffraction data [22]. In this work, the theoretical discussions are focused on our phase diagram from magnetic susceptibility measurements and the inherent mechanism. To do this, two important points are addressed in the discussion. First, in the hydrogen sulfur system, the sample shows a complex superconducting behavior at high pressures with a change in both crystal structure and stoichiometry. It is almost impossible to determine the complex superconducting behavior only through experimental techniques, as reported in the previous experiment by Drozdov *et al.* [15]. Therefore, the crystal structure and stoichiometry of the hydrogen sulfur system under high pressure have been analyzed by the reported first-principles calculations based on density functional theory (DFT). It is well known that H_2S is the only known stable compound in the H–S system at ambient pressure. We have predicted that H_2S is stable below 43 GPa and decomposes into H_3S and S above this pressure [24].

Except for H_3S, other hydrogen-rich stoichiometries were also reported to be stable above 100 GPa and the superconducting critical temperature was calculated for various H–S compounds. To compare with our experimental results, for the low-onset-temperature T_c phase below 140 GPa, the theoretically calculated T_c of the various stoichiometries H–S phase may quantitatively reproduce the low-T_c data [24,25]. It is proposed that some H–S stoichiometries may be mainly responsible for the measured superconductivity of the samples below 140 GPa. We have tried to explore the decomposition process of H_2S under high pressure and deeply understand the formation process of H_3S, through *ab initio* variable-cell molecular dynamics (MD) simulations. Our MD runs started with the orthorhombic *Pbcm* for phase III by employing a simulation cell of 96 molecules. The integrated radial distribution at 140 GPa and 100 K gives a reasonable H–S bond length with 1.76 Å. In Fig. 4, the instantaneous snapshot of polymeric networks at 140 GPa shows that an SH_6 coordinated

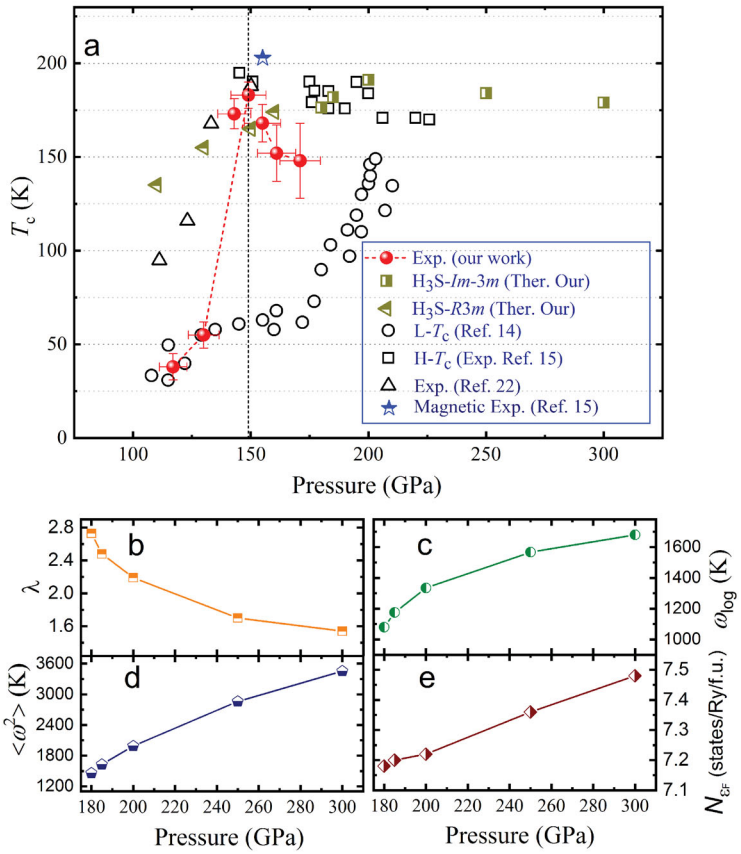

Figure 3. The measured T_c and calculated superconducting parameters at different pressures. (a) Pressure dependence of T_c in sulfur hydride. Filled circles show data from this experiment while filled squares and triangles indicate our reported theoretical work [10]. The open circles, squares and triangles show experimental results reported by Drozdov *et al.* [14,15] and Einaga *et al.* [22], respectively. The blue pentagram is obtained from the magnetic experiment by Drozdov *et al.* [15]. Lower panels show (b) the calculated parameter λ, (c) the logarithmic average phonon frequency ω_{log}, (d) the average squared phonon frequencies $\langle\omega^2\rangle$ and (e) the electronic DOS at the Fermi level $N(\varepsilon_F)$ at different pressures of the *Im*-3 *m* structure.

configuration was formed from the initial structure with increasing temperature. Under this condition, the H_2S structure exhibits extensive coordinated order and tends to adopt an SH_6 coordinated distribution as found in the cubic H_3S polymorph. Our calculation also gives average information on the H–S coordination bonds in the balanced structure during a 5 ps time scan. The detailed coordination configurations can be seen in Table S1. The coordination number of S increased significantly, which is due to the dissociation of the H_2S polymorph. The H–S bonding network adapts itself to the changing atomic distance, forming more SH_6 polymorphs.

As shown in Fig. 3a, the superconducting transition temperature T_c rises rapidly to 183 K at 149 GPa and then decreases to 140 K at 171 GPa. In the range where T_c decreases, we carried out further DFT calculations to better interpret the driving mechanism of the observed superconductivity tendency above 150 GPa. Above 150 GPa (Fig. 3a), the decrease in T_c is consistent with the formation of the *Im*-3 *m* H_3S phase predicted by our earlier theoretical calculation [10], since the predicted *R*3*m* and *Im*-3 *m* phases have different pressure dependences of T_c (Table S2, online supplementary data). The main parameters of the *Im*-3 *m* phases of H_3S at high pressures are calculated, as shown in Fig. 3b–e. The method of calculation is the same as in our previous work [10]. According to the Allen–Dynes [26] modified McMillan equation, two parameters, the electron–phonon coupling constant (EPC) λ and the logarithmic average frequency ω_{log}, control T_c. In Fig. 3b and c, the values of these parameters have been calculated for the *Im*-3 *m* phase of H_3S at high pressures. Note that λ decreases rapidly with increasing pressure, while ω_{log} has the opposite effect. As a result, the dependence of T_c on pressure is dominated by the behavior of (EPC) λ. λ can be evaluated by the formula [27]

$$\lambda = \frac{N(\varepsilon_F)\langle I^2\rangle}{M\langle\omega^2\rangle} = \frac{\eta}{M\langle\omega^2\rangle},$$

where $N(\varepsilon_F)$ is the electronic density of states at the Fermi level, $\langle I^2\rangle$ is the averaged electron–phonon matrix element, M is the mass of the atom and $\langle\omega^2\rangle$ is the average of the squared phonon frequencies. Since M is a constant, the pressure dependence of λ is determined by three parameters, $N(\varepsilon_F)$, $\langle I^2\rangle$ and $\langle\omega^2\rangle$. We have calculated $\langle\omega^2\rangle$ and $N(\varepsilon_F)$ at selected pressures, and they both increase with the application of pressure (Fig. 3d and e). As noted from the results of Papaconstantopoulos *et al.* [28], the parameter $\langle I^2\rangle$ also demonstrates a very strong pressure increase. Thus, the drop of λ may be caused only by an increase in the phonon frequency. The negative dT_c/dP is therefore mainly attributed to the decrease of λ caused by a pressure-induced hardening of the phonon frequencies.

From the plot of T_c versus pressure in Fig. 3, it should be noted that there is a difference between the superconducting critical temperatures deduced from electrical resistance data and our magnetic susceptibility measurement, and this difference increases by 30 K with increasing pressure up to 170 GPa. Still, there is no doubt that we have identified high-temperature superconductivity in the compressed sulfur hydride system from its Meissner effect. A quick overview of previous superconductivity experiments under high pressure also shows that the superconducting critical temperature observed in electrical resistance measurements is always higher than that found from magnetic susceptibility data [21,29]. For example, Li has the

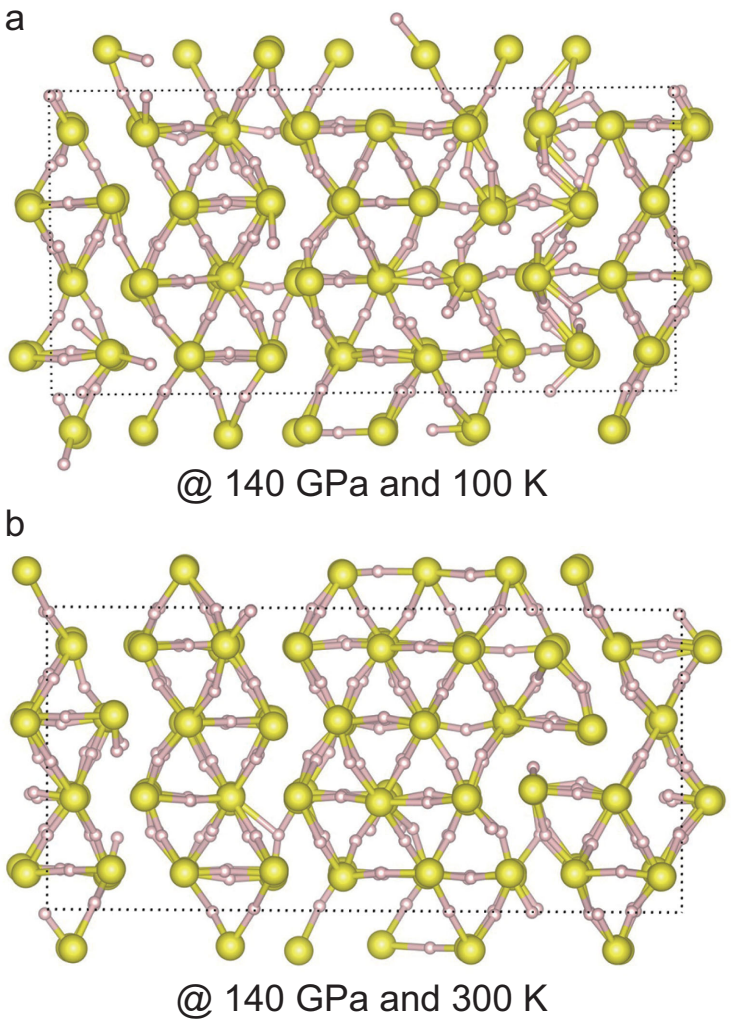

Figure 4. Snapshot of the molecular dynamics trajectory and polymeric networks of the S–H coordinated configuration. The structure views of molecular dynamics are at (a) 140 GPa and 100 K, and (b) 140 GPa and 300 K, respectively.

highest superconducting transition temperature of 14 K at 30 GPa [21], but different measurement techniques have given different phase diagrams [29,30]. Notably, the current deviation of decreasing T_c above 149 GPa can be attributed to several possible causes: (1) The magnetic measurements are sensitive to the bulk fraction of superconducting material only, whereas the resistance measurements may also react to small amounts of superconducting material inside or between grains, creating percolation paths through the material. (2) The experimental errors. In the present work, the error in the pressure is estimated from the difference between the initial and final pressures during each temperature cycle, while the error in the temperature is estimated from the difference between the onset and completion temperatures. (3) The imperfections of the samples—that the target sample contains some other sulfur hydride phases, as discussed in the above analysis. Besides, the difference of T_c data between electrical resistance and magnetic susceptibility measurement is also influenced by the compression routes, which could produce different phases of sulfur hydrides. In fact, the electrical resistance measurements by Drozdov *et al.* have obtained low-T_c and high-T_c phases with different compression routes (see Fig. 3a). The superconducting mechanism has been theoretically and experimentally confirmed as conventional type-II superconductivity consistent with the BCS scenario, and we are not able to dismiss this mechanism simply by the different slope dependences in the superconducting phase diagram. Therefore, to clearly elucidate the phenomenon and unearth the inherent physical mechanism, more experiments should be done in the future.

CONCLUSION

In summary, we present alternating-current magnetic susceptibility studies and tailor the superconducting states of the sulfur hydride system at various pressures. With increasing pressure, superconductivity appears at 38 K for 117 GPa; T_c then rises rapidly to 183 K at 149 GPa and finally decreases to 140 K at 171 GPa. An analysis of the theoretical results shows that the main causes for these variations in the superconducting transition temperature T_c are the changing stoichiometry of the hydrogen sulfur system and the drop in λ with increasing pressure. The idea of conventional high-temperature superconductivity in hydrogen-dominant compounds has thus been realized in the sulfur hydride system under hydrostatic pressure, opening further exciting perspectives for possibly realizing room-temperature superconductivity in hydrogen-based compounds.

SUPPLEMENTARY DATA

Supplementary data are available at *NSR* online.

FUNDING

This work was supported by the National Key R&D Program of China (2018YFA0305900), the National Natural Science Foundation of China (51632002, 51572108, 11504127, 11674122, 11574112, 11474127, 11634004), the 111 Project (B12011), the Program for Changjiang Scholars and Innovative Research Team in University (IRT_15R23), and the National Found for Fostering Talents of Basic Science (J1103202).

Conflict of interest statement. None declared.

REFERENCES

1. Onnes HK. The superconductivity of mercury. *Comm Phys Lab Univ Leiden* 1911; **122**: 124.
2. Ashcroft NW. Metallic hydrogen: a high-temperature superconductor? *Phys Rev Lett* 1968; **21**: 1748–9.
3. Ashcroft NW. Hydrogen dominant metallic alloys: high temperature superconductors? *Phys Rev Lett* 2004; **92**: 187002.
4. Jin X, Meng X and He Z *et al.* Superconducting high-pressure phases of disilane. *Proc Natl Acad Sci USA* 2010; **107**: 9969–73.
5. Eremets MI, Trojan IA and Medvedev SA *et al.* Superconductivity in hydrogen dominant materials: silane. *Science* 2008; **319**: 1506–9.
6. Gao G, Oganov AR and Li P *et al.* High-pressure crystal structures and superconductivity of stannane (SnH_4). *Proc Natl Acad Sci USA* 2010; **107**: 1317–20.
7. Wang H, Tse JS and Tanaka K *et al.* Superconductive sodalite-like clathrate calcium hydride at high pressures. *Proc Natl Acad Sci USA* 2012; **109**: 6463–6.
8. Zhou D, Jin X and Meng X *et al.* Ab initio study revealing a layered structure in hydrogen-rich KH_6 under high pressure. *Phys Rev B* 2012; **86**: 014118.
9. Strobel TA, Somayazulu M and Hemley RJ. Novel pressure-induced interactions in silane-hydrogen. *Phys Rev Lett* 2009; **103**: 065701.
10. Duan D, Liu Y and Tian F *et al.* Pressure-induced metallization of dense $(H_2S)_2H_2$ with high-T_c superconductivity. *Sci Rep* 2015; **4**: 6968.
11. Bednorz JG and Müller KA. Possible high T_c superconductivity in the Ba–La–Cu–O system. *Z Phys B Condens Matter* 1986; **64**: 189–93.
12. Gao L, Xue YY and Chen F *et al.* Superconductivity up to 164 K in $HgBa_2Ca_{m-1}Cu_mO_{2m+2+\delta}$ (m = 1, 2 and 3) under quasihydrostatic pressures. *Phys Rev B* 1994; **50**: 4260–3.
13. Bianconi A and Jarlborg T. Superconductivity above the lowest Earth temperature in pressurized sulfur hydride. *EPL* 2015; **112**: 37001.
14. Drozdov AP, Eremets MI and Troyan IA. Conventional superconductivity at 190 K at high pressures. arXiv:1412.0460.
15. Drozdov AP, Eremets MI and Troyan IA *et al.* Conventional superconductivity at 203 kelvin at high pressures in the sulfur hydride system. *Nature* 2015; **525**: 73–6.
16. Duan D, Liu Y and Tian F *et al.* Pressure-induced decomposition of solid hydrogen sulfide. *Phys Rev B* 2015; **91**: 180502.
17. Tateiwa N, Haga Y and Fisk Z *et al.* Miniature ceramic-anvil high-pressure cell for magnetic measurements in a commercial superconducting quantum interference device magnetometer. *Rev Sci Instrum* 2011; **82**: 053906.
18. Troyan I, Gavriliuk A and Rüffer R *et al.* Observation of superconductivity in hydrogen sulfide from nuclear resonant scattering. *Science* 2016; **351**: 1303–6.
19. Timofeev YA, Struzhkin VV and Hemley RJ *et al.* Improved techniques for measurement of superconductivity in diamond anvil cells by magnetic susceptibility. *Rev Sci Instrum* 2002; **73**: 371–7.
20. Gregoryanz E, Struzhkin VV and Hemley RJ *et al.* Superconductivity in the chalcogens up to multimegabar pressures. *Phys Rev B* 2002; **65**: 064504.
21. Deemyad S and Schilling JS. Superconducting phase diagram of Li metal in nearly hydrostatic pressures up to 67 GPa. *Phys Rev Lett* 2003; **91**: 167001.
22. Einaga M, Sakata M and Shikawa T *et al.* Crystal structure of the superconducting phase of sulfur hydride. *Nat Phys* 2016; **12**: 835–8.
23. Struzhkin VV, Hemley RJ and Mao HK *et al.* Superconductivity at 10–17 K in compressed sulphur. *Nature* 1997; **390**: 382–4.
24. Li Y, Hao J and Liu H *et al.* The metallization and superconductivity of dense hydrogen sulfide. *J Chem Phys* 2014; **140**: 174712.
25. Ishikawa T, Nakanishi A and Shimizu K *et al.* Superconducting H_5S_2 phase in sulfur-hydrogen system under high-pressure. *Sci Rep* 2016; **6**: 23160.
26. Allen PB and Dynes RC. Transition temperature of strong-coupled superconductors reanalyzed. *Phys Rev B* 1975; **12**: 905–22.
27. McMillan WL. Transition temperature of strong-coupled superconductors. *Phys Rev* 1968; **167**: 331–44.
28. Papaconstantopoulos DA, Klein BM and Mehl MJ *et al.* Cubic HS around 200 GPa: an atomic hydrogen superconductor stabilized by sulfur. *Phys Rev B* 2015; **91**: 184511.
29. Shimizu K, Ishikawa H and Takao D *et al.* Superconductivity in compressed lithium at 20 K. *Nature* 2002; **419**: 597–9.
30. Schaeffer AM, Temple SR and Bishop JK *et al.* High-pressure superconducting phase diagram of ^{6}Li: isotope effects in dense lithium. *Proc Natl Acad Sci USA* 2015; **112**: 60–4.